Tuijin Jishu/Journal of Propulsion Technology
ISSN: 1001-4055
Vol. 45 No. 2 (2024)

Numerical Simulation of Three-Dimensional Free Surface Fluid Sloshing with ALE Finite Element Method

Bhanu Teja · Shweta Srivastava*

Department of Computational and Data Sciences, Indian Institute of Science, Bangalore, India, 560012

** Digital University Kerala, Technocity Campus, Thiruvananthapuram, Kerala, India, 695317*

Abstract:- This paper presents the methodology for the simulation of free surface fluid sloshing. Particularly the nu- merical solution of the fluid flow i.e., Navier-Stokes equations which is posed in a moving mesh framework is presented. The time-changing nature of the domain is handled by the arbitrary Lagrangian-Eulerian (ALE) framework. The govern- ing equations are discretized with the finite element method. A fixed point iteration technique is used for linearizing the resultant set of non-linear algebraic equations. A fully implicit one-step scheme is used for time stepping. For the mesh movement, a linear elastic model is used which is known to preserve the mesh quality. The stability estimates for the semi-discrete and fully discrete scheme are analyzed. The methodology is assessed through the simulation of fluid sloshing in a rectangular tank with an initial uneven surface. The methodology is shown to result in stable simulations for many time steps. The conservation of mass and other physical parameters along with numerical parameters are presented.

Keywords*: Navier-Stokes equation, Arbitrary Lagrangian Eulerian formulation, Moving mesh method, Implicit Euler discretization, Stability estimates, Free surface fluid sloshing*

1. Introduction

Free surface flows are ubiquitous in nature and industry. Unlike flows in full enclosures such as pipes, free surface flows are fluid flows where a part or complete(for example: droplets) por- tion of the fluid boundary is exposed to another phase such as gas or vacuum. Flows in rivers, oceans, laboratory towing tanks, flows past floating objects, bridge piers and fluid droplets in air/gas are examples of free surface flows. Simulation of free surface flows is particularly chal- lenging as the physical space occupied by the fluid and thus the computational domain itself changes with time. These types of flow problems are generally called free boundary problems (or) interface/multiphase flow problems.

The difficulties inherent in these problems are very challenging for mathematical and com- putational analyses. From the mathematical point of view, one has to appropriately model the free boundary kinematics and solve the strong coupling between the boundary motion and the dynamics of the continuum. From the computational point of view and in the discrete setting, one has to correctly choose the discretization parameters, coupling, and solution algorithms for a stable and accurate solution.

Tracking or capturing the interface, accurately incorporating the boundary conditions on the interface, and guaranteeing mass conservation are some of the challenges in interface flow computations. It turns out that the development of robust and efficient numerical schemes for computing fluid flows with unsteady motion of moving interfaces is a challenging problem in the computational fluid dynamics(CFD) field[10].

Several techniques have been proposed in the literature to capture/track interfaces, see for an overview [13]. Based on how the interface is captured, all these techniques can be classified into two classes: (i) fixed grid and (ii) moving grid methods. Each method has its own advantages and disadvantages. Among the fixed grid techniques, Marker-and-cell(MAC)[17], Volume- of-Fluid(VOF)[15], Level Set(LS)[19] and Front-Tracking(FT)[13] are a

few popular techniques. The MAC method, where marker particles are used to identify each fluid, is the oldest and most popular method for computing multiphase flows. In the VOF method, a 'volume-of-fluid or marker function' is used to identify each fluid phase. The 'volume-of-fluid' function gives the volume fraction of one of the fluids in each of the cells of the discretized domain. Another popular and very flexible method is the Level Set method, which was introduced by Osher and Sethian. In this Eulerian kinematic description or fixed grid-based method, the actual position of the free boundary is localized in a fixed mesh. The equations of the fluid are solved in a larger domain than that really occupied by the fluid. The interface between various phases has to be distinguished by the characteristic function (the 'volume-of-fluid marker function' or the 'level-set function'). In principle, these methods can be employed for general free and moving boundary problems, however, the identification of the interface needs a refined mesh in order to obtain sufficient accuracy. Another popular method in dealing with PDEs in time-changing domains is the Arbitrary Lagrangian Eulerian(ALE) formulation which is used in this study. An early description of the approach is given in [9]. In this approach, the governing equations are posed in a moving mesh framework. The interface/boundary is resolved by the mesh and moves with the fluid in a Lagrangian way. The inner mesh points can be displaced in an arbitrarily prescribed way. This avoids quick distortion of mesh [4]. Since the boundary is resolved by the mesh in the ALE approach, the inclusion of boundary conditions in the solution process is straightforward [10].

One main drawback of the ALE or moving mesh method is the need for re-meshing when the mesh is too distorted or the quality of mesh(indicated by a metric) is too low during the course of the simulation. This re-meshing of the computational domain and interpolation of quantities of interest to the new mesh from the old mesh is computationally expensive. Also for three-dimensional and realistic meshes, re-meshing algorithms are almost nonexistent. But as the interface is resolved, accurate representation of the dynamics of the free surface is possible for not too large topological changes. This gives the ALE method a powerful advantage in mass conservation. As mentioned, the method fails when there are large topological changes such as overturning of waves, splitting and merging of fluid, etc. Whereas interface-capturing methods can capture large topological changes but the interface cannot be represented accurately which leads to mass conservation problems.

In this study, we choose the ALE concept for the kinematic description, a linear elastic model for mesh movement which is known to conserve mesh quality better than harmonic extension[10], the finite element method for space discretization, an implicit Euler method for time discretiza- tion and finally all the equations are solved in a coupled fashion. The primary unknowns are the fluid velocity, the pressure, and the mesh velocity. Our contribution in the present paper concerns the following important issues: the finite element discretization of the coupled system of governing equations, a fully implicit Euler time-stepping scheme, the use of fixed point iteration technique to deal with nonlinearity, analyzing stability estimates for both semi-discrete and fully discrete scheme in moving mesh problems and establishment of benchmark tests to easily validate the code.

It is, indeed, well known that when discretizing the Galerkin formulation of the Navier- Stokes equations, care should be exercised to avoid undesirable oscillations for pressure in the low Reynolds regime and for the whole system in the advection-dominated regime. The first kind of instabilities can be avoided by choosing compatible velocity and pressure finite element approximations, i.e. to satisfy the inf-sup condition [23], [4]. Whereas in the latter case, insta- bilities can be avoided by adding some diffusive mechanisms such as the effect induced in the streamline Petrov Galerkin method and Galerkin Least Squares method [18]. Our study for the paper pertains to the former, the low Reynolds regime. Hence stabilization techniques for high Reynolds/advection dominated regime are not discussed.

The rest of the paper is arranged as follows: Section 2 presents the governing equations in ALE formulation. Section 3 presents the function spaces and the weak form of the equations. Further, the finite element discretization and stability estimates of the semi-discrete scheme are analyzed in Section 4. Section 5 presents the time stepping and stability of the fully discrete scheme. Implementation aspects and numerical results are presented in section 6. Finally, the observations and conclusions are presented in section 7.

2. Governing Equations

The Navier-Stokes equations for an incompressible fluid in a time-dependent domain $\Omega(t) \subset R^3$, together with the force balancing boundary conditions on the free surface $\Gamma_F(t) \subset \partial\Omega(t)$ and no penetration free slip boundary conditions on $\Gamma_W(t) = \partial\Omega(t)/\Gamma_F(t)$ are given by

$$\frac{\partial u}{\partial t} + (\boldsymbol{u} \cdot \nabla)u - \frac{1}{\rho}\nabla \cdot T(\boldsymbol{u}, p) = \boldsymbol{g} \qquad in\ \Omega(t) \times [0, I]$$

$$\nabla \cdot \boldsymbol{u} = 0 \qquad in\ \Omega(t) \times [0, I]$$

$$-T \cdot n = r \qquad \Gamma_F(t) \times [0, I] \qquad (1)$$

$$u \cdot n = 0 \qquad \Gamma_W(t) \times [0, I]$$

$$\tau_i \cdot T \cdot n = 0 \qquad for\ i = 1,2\ on(t) \times [0, I]$$

where **u**, p, ρ, t, **r**, $\boldsymbol{\tau}$, $\boldsymbol{n}$ and I denote the fluid velocity, pressure, fluid density, time, external traction, unit tangent, outward unit normal and given end time respectively. Here, the stress tensor $T(u, p)$ is given by

$$T(\boldsymbol{u}, p) = -pI + 2\mu D(\boldsymbol{u}) \qquad (2)$$

where I and μ denote the identity tensor and the dynamic viscosity of the fluid respectively. Further, the velocity deformation tensor $D(\boldsymbol{u})$ is given by

$$D(\boldsymbol{u}) = \frac{1}{2}(\nabla \boldsymbol{u} + \nabla \boldsymbol{u}^T)$$

where the superscript T denotes transpose. Further, the kinematic condition

$$\boldsymbol{w} \cdot n = \boldsymbol{u} \cdot n \quad on\ \Gamma_F(t) \times [0, I]$$

on the free surface has to be satisfied, i.e., the normal velocity of the interface should be equal to the normal velocity of the fluid(at the interface). Here **w** is the interface velocity. In addition, the initial condition and initial domain have to be specified i.e., $\mathbf{u}(\mathbf{x}, 0) = \mathbf{u}_0(\mathbf{x})$ and $\Omega(0)$. For our computations in section 6, we use $\mathbf{u}_0(\mathbf{x}) = 0$ i.e., the fluid is at rest at time $t = 0$. The computational domain used in the study is shown in figure 1.

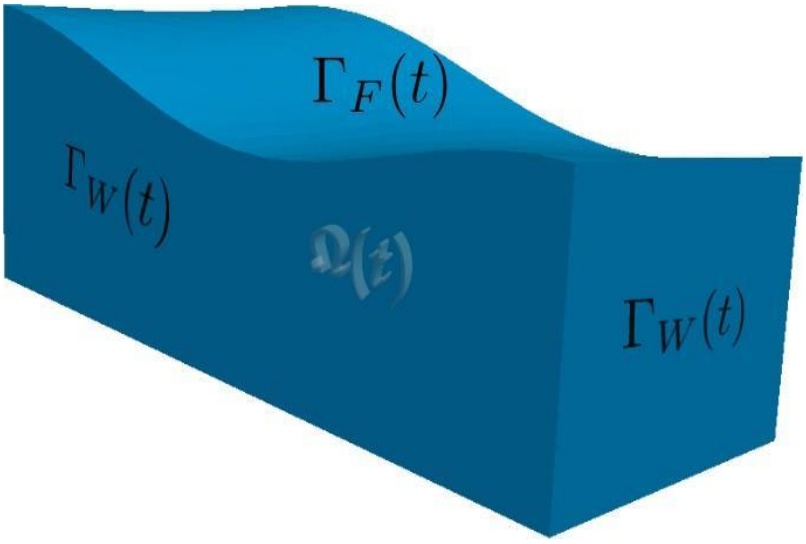

Fig..1 Computational domain at t = 0 for free surface fluid sloshing simulation

2.1 Slip with friction boundary condition

The free slip boundary condition that the velocity of the liquid relative to the solid surface at the liquid-solid interface is an assumption. It is known that these frictional effects will not affect the macroscopic flow profile of

the fluid in bulk fluid flows. As we are dealing with macroscopic or bulk fluid flow, this assumption is justified. Whereas in microfluidics, these frictional effects at interfaces strongly influence flow dynamics. The slip with friction or Navier-slip boundary condition is given as

$$u \cdot n = 0, \quad \boldsymbol{u} \cdot \tau_i = -\epsilon_\mu(\tau_i \cdot T(\boldsymbol{u}, p) \cdot n), \quad on\ \Gamma_W(t) \times [0, I] \tag{3}$$

For i = 1, ..., d-1, where d is the dimension of the considered problem. ϵ_μ is the slip coefficient. The unit of stress in SI units is $kg/m.s^2$ and the velocity is m/s. So the unit of slip coefficient ϵ_μ is velocity/unit stress. The first condition in (3) is the no penetration boundary condition, that is the fluid cannot penetrate an impermeable solid boundary and thus the normal component of the velocity is zero. The second condition is the slip with friction boundary condition, that is at the liquid-solid interface, the tangential velocities of the fluid are proportional to their corresponding tangential stresses. Depending on the choice of ϵ, one gets different boundary conditions as follows.

1. no-slip if $\epsilon = 0$
2. slip with friction if $0 < \epsilon < \infty$
3. free slip if $\epsilon = \infty$

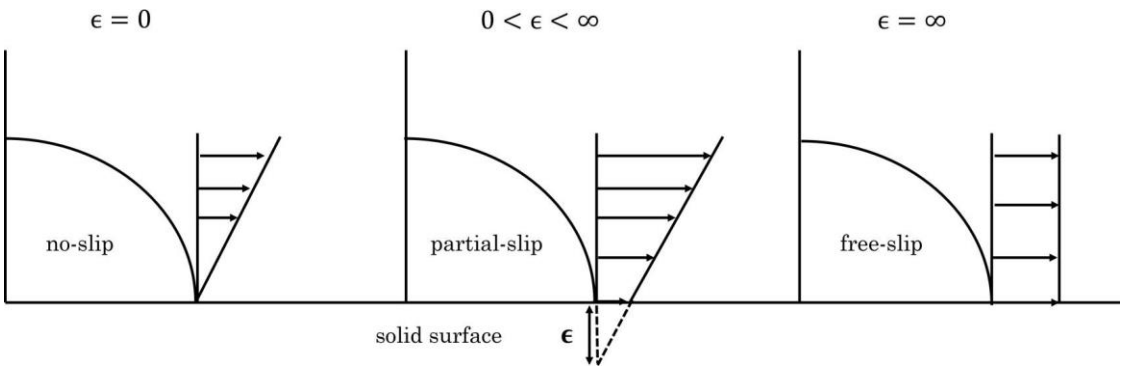

Fig...2 Interpretation of Navier slip length ϵ

For an interpretation of slip length, see Fig 2. For example, in the case of shear flow, i.e., partial slip ϵ can be interpreted as the fictitious distance to the solid surface as shown in Fig 2(second). For a more detailed description of the slip boundary condition, see [5]. In the present paper, we have considered an impervious and free slip boundary condition at the fluid-solid interface(walls) at all times. Thus $\mathbf{u} \cdot \boldsymbol{n} = 0$ and $\boldsymbol{\tau}_i \cdot \mathrm{T} \cdot \boldsymbol{n} = 0$ is the condition on $\Gamma_W(t) \times [0, \mathrm{I}]$.

2.2 Model Problem and its ALE formulation

Let the boundary points on all the interfaces be denoted by χ_F . In the ALE formulation, the boundary points χ_F are advected with their corresponding velocity as

$$\frac{d\chi_F}{dt} = u(\chi_F, t) \tag{4}$$

and the inner points are moved arbitrarily to preserve the mesh quality.

To rewrite the equation (1) in ALE form, let us define a family of mappings A_t, which at each time $t \in [0, T)$ map a point (namely ALE coordinate) $Y \in \hat{\Omega}$ of a reference domain $\hat{\Omega}$ onto a point (namely Eulerian coordinate) $\mathbf{X}$ of the current domain Ω_t. That is,

$$A_t : \hat{\Omega} \rightarrow \Omega_t, \quad A_t(Y) = X(Y, t)$$

for each $t \in [0, T)$. We assume that the mapping A_t is a homeomorphic function i.e, $A_t \in C^0(\underline{\hat{\Omega}})$. Furthermore, we assume the mapping

$$t \to X(Y,t), \qquad Y \in \hat{\Omega}$$

Is differentiable almost everywhere in [0,T).

The function **v** in (1) is defined on the Eulerian frame. Here we define

The function **v** in (1) is defined on the Eulerian frame. Here we define

$$\hat{\mathbf{v}} := \mathbf{v} \circ \mathcal{A}_t, \quad \hat{v} : \hat{\Omega} \times (0,\mathrm{T}) \to \mathbb{R}, \quad \hat{\mathbf{v}}(\mathbf{Y},t) = \mathbf{v}(\mathcal{A}_t(\mathbf{Y}),t),$$

which is the corresponding function on the ALE frame. Furthermore, the time derivative of **v** on the ALE frame is given by

$$\left.\frac{\partial \mathbf{v}}{\partial t}\right|_{\hat{\Omega}} : \Omega_t \times (0,\mathrm{T}) \to \mathbb{R}, \quad \left.\frac{\partial \mathbf{v}}{\partial t}\right|_{\hat{\Omega}}(\mathbf{X},t) = \frac{\partial \hat{\mathbf{v}}}{\partial t}(\mathbf{Y},t), \quad \mathbf{Y} = \mathcal{A}_t^{-1}(\mathbf{X}),$$

Here $|_{\hat{\Omega}}$ is used to indicate the time derivative is on the ALE frame. Further, the time derivative on the Eulerian frame is indicated by $|_X$. The domain velocity **w** is defined by

$$\boldsymbol{w}(\boldsymbol{X},t) = \frac{\partial X}{\partial t}|_{\hat{\Omega}}$$

Now to get $\frac{\partial \hat{v}}{\partial t} = \frac{\partial v}{\partial t}|_{\hat{\Omega}}$, i.e., the time derivative of $\hat{v}$, we apply total derivative to the composition v $\circ$ A_t to obtain

$$\left.\frac{\partial \mathbf{v}}{\partial t}\right|_{\hat{\Omega}} = \left.\frac{\partial \mathbf{v}}{\partial t}\right|_{\mathbf{X}} + \left.\frac{\partial \mathbf{X}}{\partial t}\right|_{\hat{\Omega}} \cdot \nabla_{\mathbf{X}}\mathbf{v} = \left.\frac{\partial \mathbf{v}}{\partial t}\right|_{\mathbf{X}} + \mathbf{w} \cdot \nabla_{\mathbf{X}}\mathbf{v}, \tag{5}$$

where ∇_X denotes the gradient with respect to the Eulerian coordinate (this is qualitatively and quantitatively the same as normal space gradient as space gradients are not influenced by mesh velocity). Using the above relation (5) in the equation (1), we get

$$\begin{aligned}
\frac{\partial \mathbf{u}}{\partial t} + ((\mathbf{u}-\mathbf{w})\cdot\nabla)\mathbf{u} - \frac{1}{\rho}\nabla\cdot\mathbb{T}(\mathbf{u},p) &= \mathbf{g} && \text{in } \Omega(t)\times[0,\mathrm{I}] \\
\nabla\cdot\mathbf{u} &= 0 && \text{in } \Omega(t)\times[0,\mathrm{I}] \\
\mathbb{T}\cdot\boldsymbol{n} &= \mathbf{r} && \text{on } \Gamma_F(t)\times[0,\mathrm{I}] \\
\mathbf{u}\cdot\boldsymbol{n} &= 0 && \text{on } \Gamma_W(t)\times[0,\mathrm{I}] \\
\boldsymbol{\tau}_i\cdot\mathbb{T}\cdot\boldsymbol{n} &= 0 && \text{for i=1,2 on } \Gamma_W(t)\times[0,\mathrm{I}]
\end{aligned} \tag{6}$$

The extra term $-w \cdot \nabla_X v$ can be interpreted as a correction in the actual time gradient of the quantity **v** because of the extra unphysical time gradient induced by mesh movement.

2.3 Linear elastic model for mesh movement/velocity

Given the free surface boundary displacement/velocity, the interior points can be moved based on the linear elastic model. It is known that the linear elastic model preserves the mesh quality better than harmonic extension [10]. The model is given by

$$\begin{aligned}
\nabla\cdot\mathbb{S}(\mathbf{w}) &= 0 && \text{in } \Omega(t)\times[0,\mathrm{I}] \\
\text{with } \mathbf{w}\cdot\boldsymbol{n} &= \mathbf{u}\cdot\boldsymbol{n} && \text{on } \Gamma_F(t)\times[0,\mathrm{I}] \\
\mathbf{w}\cdot\boldsymbol{n} &= 0 && \text{on } \Gamma_W(t)\times[0,\mathrm{I}] \\
\boldsymbol{\tau}_i\cdot\mathbb{D}(\mathbf{w})\cdot\boldsymbol{n} &= 0 \quad \text{for i=1, 2} && \text{on } \Gamma_W(t)\times[0,\mathrm{I}]
\end{aligned} \tag{7}$$

$$\text{where } \mathbb{S}(\mathbf{w}) = \lambda_1(\nabla\cdot\mathbf{w})\mathbb{I} + 2\lambda_2\mathbf{D}(\mathbf{w})$$

Here **w** is the mesh velocity, λ_1 and λ_2 are called Lamé constants and for the present computations

they are taken as $\lambda_1 = \lambda_2 = 1$. Also no ALE mapping is required for mesh movement as it is treated in Lagrangian way.

2.4 NSE-ALE equation coupled with linear elastic model

Here we write equation (6) in 2.2 coupled with linear elastic model

$$\begin{aligned} \frac{\partial \mathbf{u}}{\partial t} + ((\mathbf{u}-\mathbf{w})\cdot\nabla)\mathbf{u} - \frac{1}{\rho}\nabla\cdot\mathbb{T}(\mathbf{u},p) &= \mathbf{g} \quad \text{in } \Omega(t)\times[0,\mathrm{I}] \\ \nabla\cdot\mathbf{u} &= 0 \quad \text{in } \Omega(t)\times[0,\mathrm{I}] \\ \nabla\cdot\mathbb{S}(\mathbf{w}) &= 0 \quad \text{in } \Omega(t)\times[0,\mathrm{I}] \end{aligned} \tag{8}$$

with the boundary conditions and initial conditions as

$$\begin{aligned} -\mathbb{T}\cdot\boldsymbol{n} &= \mathbf{r} && \text{on } \Gamma_F(t)\times[0,\mathrm{I}] \\ \mathbf{u}\cdot\boldsymbol{n} &= 0 && \text{on } \Gamma_W(t)\times[0,\mathrm{I}] \\ \boldsymbol{\tau}_i\cdot\mathbb{T}\cdot\boldsymbol{n} &= 0 \quad \text{for } i=1,2 && \text{on } \Gamma_W(t)\times[0,\mathrm{I}] \\ \mathbf{w}\cdot\boldsymbol{n} &= \mathbf{u}\cdot\boldsymbol{n} && \text{on } \Gamma_F(t)\times[0,\mathrm{I}] \\ \mathbf{w}\cdot\boldsymbol{n} &= 0 && \text{on } \Gamma_W(t)\times[0,\mathrm{I}] \\ \boldsymbol{\tau}_i\cdot\mathbb{D}(\mathbf{w})\cdot\boldsymbol{n} &= 0 \quad \text{for } i=1,2 && \text{on } \Gamma_W(t)\times[0,\mathrm{I}] \\ \mathbf{u}(\mathbf{x},0) = \ \mathbf{u}_0(\mathbf{x}) &= 0 && \text{in } \Omega(0) \end{aligned} \tag{9}$$

3. Governing Variational form of the NSE-ALE equation

To derive the weak formulation of the governing equations (8) with the boundary conditions (9), we define solution and test spaces

$$V_{\mathcal{A}}(\Omega_t) = \left\{\mathbf{v}:\Omega_t\times(0,\mathrm{I})\to\mathbb{R}^3, \mathbf{v}=\hat{\mathbf{v}}\circ\mathcal{A}_t^{-1}, \hat{\mathbf{v}}\in \mathrm{H}^1(\hat{\Omega})\right\}$$
$$V_{\mathcal{A},0}(\Omega_t) = \left\{\mathbf{v}:\Omega_t\times(0,\mathrm{I})\to\mathbb{R}^3, \mathbf{v}=\hat{\mathbf{v}}\circ\mathcal{A}_t^{-1}, \mathbf{v}\cdot\boldsymbol{n}=0 \text{ on } \Gamma_W, \hat{\mathbf{v}}\in \mathrm{H}_0^1(\hat{\Omega})\right\}$$

for velocity, where

$$\begin{aligned} \mathrm{H}_0^1(\hat{\Omega}) &= \left\{\hat{\mathbf{v}}:\hat{\Omega}\to\mathbb{R}^3, \hat{\mathbf{v}}\cdot\boldsymbol{n}=0 \text{ on } \hat{\Gamma}_W, \hat{\mathbf{v}}\in \mathrm{H}^1(\hat{\Omega})\right\} \\ \text{and} \\ Q_{\mathcal{A}}(\Omega_t) &= \left\{q:\Omega_t\times(0,\mathrm{I})\to\mathbb{R}, q=\hat{q}\circ\mathcal{A}_t^{-1}, \hat{q}\in L_2(\hat{\Omega})\right\} \end{aligned} \tag{10}$$

pressure, and

$$S(\Omega_t) = \left\{\mathbf{s}:\Omega_t\times(0,\mathrm{I})\to\mathbb{R}^3, \mathbf{s}\in H^1(\Omega_t)\right\}$$
$$S_0(\Omega_t) = \left\{\mathbf{s}:\Omega_t\times(0,\mathrm{I})\to\mathbb{R}^3, \mathbf{s}=0 \text{ on } \partial\Omega_t\right\}$$

for linear elastic model for mesh movement.

The $v = \hat{v}\circ A_t^{-1}$ in velocity space and similar composition in pressure space essentially means the (basis)functions in the current domain i.e, $\boldsymbol{v}\in\Omega_t$ are obtainable by composition of (ba- sis)functions in reference domain i.e, $\hat{\boldsymbol{v}}\in\hat{\Omega}_t$ with ALE mapping, and no such mapping or ALE transformation is required for mesh movement as it is treated in the Lagrangian way.

Moreover, the L^2–inner product, the norm and the semi-norm, $(\cdot,\cdot)_t$, $\|\cdot\|_{0,t}$ and $|\cdot|_{1,t}$, respectively, over Ω_t are defined as

$$(\mathbf{u},\mathbf{v})_t := \int_{\Omega_t} \mathbf{u}\mathbf{v}\, dx, \qquad \|\mathbf{v}\|^2_{0,t} := (\mathbf{v},\mathbf{v})_t, \qquad |\mathbf{v}|^2_{1,t} := (\nabla\mathbf{v},\nabla\mathbf{v})_t\,, \qquad \forall\ \mathbf{u},\mathbf{v} \in V_{\mathcal{A}}(\Omega_t).$$

Thus the weak form for NSE-ALE equation coupled with linear elastic model reads: Find $\mathbf{u} \in V_A(\Omega_t)$, $p \in Q_A(\Omega_t)$ and $\mathbf{w} \in S(\Omega_t)$ such that

$$\int_{\Omega(t)} \left.\frac{\partial \mathbf{u}}{\partial t}\right|_{\hat{\Omega}} \cdot \mathbf{v}\ dx + \int_{\Omega(t)} ((\mathbf{u}-\mathbf{w})\cdot\nabla)\mathbf{u}\cdot\mathbf{v}\ dx - \frac{1}{\rho}\int_{\Omega(t)} \nabla\cdot\mathbb{T}(\mathbf{u},p)\cdot\mathbf{v}\ dx = \int_{\Omega(t)} \mathbf{g}\cdot\mathbf{v}\ dx,\ \forall \mathbf{v} \in V_{\mathcal{A},0}(\Omega_t)$$

$$\int_{\Omega(t)} (\nabla\cdot\mathbf{u})q\ dx = 0,\quad \forall\ q \in Q_{\mathcal{A}}(\Omega_t),$$

$$\int_{\Omega(t)} \nabla\cdot\mathbb{S}\cdot\mathbf{w}\ dx = 0,\quad \forall\ \mathbf{s} \in S_0(\Omega_t).$$

Applying integration by parts to the stress tensor term in the weak form of momentum equation and applying boundary conditions gives.

$$-\frac{1}{\rho}\int_{\Omega(t)} \nabla\cdot\mathbb{T}(\mathbf{u},p)\cdot\mathbf{v}\ dx = -\frac{1}{\rho}\left[-\int_{\Gamma_F} \mathbf{v}\cdot\mathbf{r}\ d\Gamma_F - \int_{\Omega(t)} \mathbb{T}(\mathbf{u},p) : \mathbb{D}(\mathbf{v})\ dx\right]$$

The complete derivation is given in appendix A.

Following a similar procedure of applying integration by parts to the symmetric tensor term in the weak form of the linear elastic model. The weak form reads: Find $\mathbf{w} \in S(\Omega_t)$ such that

$$\lambda_1 \int_{\Omega(t)} \nabla\cdot\mathbf{w}\nabla\cdot\mathbf{s}\ dx - 2\lambda_2 \int_{\Omega(t)} \mathbb{D}(\mathbf{w}) : \mathbb{D}(\mathbf{s})\ dx = 0,\quad \forall\ \mathbf{s} \in S_0(\Omega_t). \tag{11}$$

The application of integration by parts is elaborated in appendix B. Putting it all together, thus after applying integration by parts, the weak form of Navier-Stokes equations in ALE form coupled with linear elastic model reads: Find $\mathbf{u} \in V_A(\Omega_t)$, $p \in Q_A(\Omega_t)$, and $\mathbf{w} \in S(\Omega_t)$ such that

$$\int_{\Omega(t)} \left.\frac{\partial \mathbf{u}}{\partial t}\right|_{\hat{\Omega}} \cdot \mathbf{v}\ dx + \int_{\Omega(t)} ((\mathbf{u}-\mathbf{w})\cdot\nabla)\mathbf{u}\cdot\mathbf{v}\ dx + \frac{1}{\rho}\left[2\mu\int_{\Omega(t)} \nabla_x(\mathbf{u}) : \mathbb{D}(\mathbf{v})\ dx - \int_{\Omega(t)} (\nabla_x\cdot\mathbf{v})\ p\ dx\right]$$

$$= \int_{\Omega(t)} \mathbf{g}\cdot\mathbf{v}\ dx - \frac{1}{\rho}\int_{\Gamma_F} \mathbf{v}\cdot\mathbf{r}\ dx,\quad \forall\ \mathbf{v} \in V_{\mathcal{A},0}(\Omega_t),$$

$$\int_{\Omega(t)} (\nabla\cdot\mathbf{u})q\ dx = 0,\quad \forall\ q \in Q_{\mathcal{A}}(\Omega_t),$$

$$\lambda_1 \int_{\Omega(t)} (\nabla\cdot\mathbf{w})(\nabla\cdot\mathbf{s})\ dx - 2\lambda_2 \int_{\Omega(t)} \mathbb{D}(\mathbf{w}) : \mathbb{D}(\mathbf{s})\ dx = 0,\quad \forall\ \mathbf{s} \in S_0(\Omega_t). \tag{12}$$

with the boundary and initial conditions specified in (9).

Remark: The quantity $\frac{1}{\rho}\int_{\Gamma_F} v\cdot r$ is a known quantity and is taken to RHS in the system matrix assembly process.

We will utilize an important inequality known as Korn's inequality, which states that:

$$\int_{\Omega(t)} \mathbb{D}(\mathbf{u}) : \mathbb{D}(\mathbf{u})\ dx \geq C_0(\Omega_t)\ ||\nabla\cdot\mathbf{u}||^2_{L^2(\Omega_t)},\quad \forall \mathbf{u} \in [H^1(\Omega_t)]^d, \tag{13}$$

where $C_0(\Omega_t)$ is a positive constant, whose value depends on Ω_t.

Lemma 1 *Let* $\mathbf{u} = \mathbf{u}(\mathbf{x}, t)$ *be the divergence free velocity, that is* $\nabla \cdot \mathbf{u} = 0$, *in a time varying domain* $\Omega t \in R^2$ *and* $\Gamma(t) = \partial\Omega_t$. *Let* $\boldsymbol{n}$ *be the outward unit normal vector on* $\Gamma(t)$, *then,*

$$\frac{d\mathbf{X}}{dt} = \mathbf{u}(\mathbf{X}, t), \ \mathbf{X}(0, s) = \mathbf{X}_0(s), \ s \in P \tag{14}$$

and

$$\frac{d\mathbf{X}^*}{dt} = (\mathbf{u}(\mathbf{X}^*, t) \cdot \boldsymbol{n})\boldsymbol{n}, \ \mathbf{X}^*(0, s) = \mathbf{X}_0(s), \ s \in P \tag{15}$$

where P is a set of parameters, are equivalent and both preserve volume of Ω_t

Proof. The solution of (14) gives a parametrization of Γ (t) as

$$x = x(t, s), y = y(t, s), \ s \in P \ \ \forall \ \ \mathbf{X} = (x, y) \in \Gamma(t) \tag{16}$$

The volume of Ω_t is

$$|\Omega_t| = \frac{1}{2}\int_{\Gamma(t)} xdy - ydx = \frac{1}{2}\int_{s\in P}\left\{x(t,s)\frac{\partial y}{\partial s}(t,s) - y(t,s)\frac{\partial x}{\partial s}(t,s)\right\}ds \tag{17}$$

Now, take the time derivative and use(14) to get

$$\begin{aligned}\frac{d}{dt}|\Omega_t| &= \frac{1}{2}\int_{s\in P}\left\{u_1\frac{\partial y}{\partial s} - u_2\frac{\partial x}{\partial s} + x\frac{\partial^2 y}{\partial s\partial t} - y\frac{\partial^2 x}{\partial s\partial t}\right\}ds \\ &= \frac{1}{2}\int_{s\in P}\left\{u_1\frac{\partial y}{\partial s} - u_2\frac{\partial x}{\partial s} + x\frac{\partial u_2}{\partial s} - y\frac{\partial u_1}{\partial s}\right\}ds \\ &= \frac{1}{2}\int_{s\in P}\left\{2\left(u_1\frac{\partial y}{\partial s} - u_2\frac{\partial x}{\partial s}\right) + \frac{\partial}{\partial s}(xu_2 - yu_1)\right\}ds\end{aligned} \tag{18}$$

The first term in the above integral vanishes, since

$$0 = \int_{\Omega_t}\nabla\cdot\mathbf{u}dX = \int_{\Gamma_t}\mathbf{u}\cdot\boldsymbol{n}d\gamma = \int_{s\in P}\left(u_1\frac{\partial y}{\partial s} - u_2\frac{\partial x}{\partial s}\right)ds$$

Then we have,

$$\frac{1}{2}\int_{s\in P}\frac{\partial}{\partial s}(xu_2 - yu_1)ds = \frac{1}{2}\{x(t,s)u_2(x(t,s),y(t,s),t - y(t,s)u_1(x(t,s),y(t,s),t))\}_{s=s_0}^{s=s_1}$$

If $P \in [0, 1]$, then we have $\mathbf{X}_0(0) = \mathbf{X}_0(1)$, since $\Gamma(0)$ is a closed curve. Due to the unique solvability of (15) we conclude

$$\boldsymbol{X}(t, 1) = \boldsymbol{X}(t, 0) \ \ \forall \ t \geq 0$$

Thus, the second term also vanishes, and we get

$$\frac{d}{dt}|\Omega_t| = 0 \rightarrow |\Omega_t| = \ constant \ = |\Omega_0|$$

Now, using (15) we have to replace (18) by

$$u_1 = (\boldsymbol{u} \cdot n)n_1 \ and \ u_2 = (\boldsymbol{u} \cdot n)n_2$$

Thus, for the first term in the integral (15), we get

$$(\boldsymbol{u} \cdot n)n_1 \cdot n_1 + (\boldsymbol{u} \cdot n)n_2 \cdot n_2 = (\boldsymbol{u} \cdot n)$$

which means that the first term vanishes again. Further, the second term vanishes too, since it is independent of the velocity field. i.e., it uses only the argument of Γ_0 is closed and the unique solvability of (15). Hence both (14) and (15) are equivalent, and in the continuous model, $\nabla \cdot \mathbf{u} = 0$ in $\Omega(t)$ guarantees the conservation of volume [10].

4. Finite element discretization of the ALE equation

Let $T_{h,t}$ be the collection of simplices obtained by triangulating the time-dependent domain Ω_t. We denote the diameter of the cell $K \in T_{h,t}$ *by* $h_{K,t}$, and the global mesh size in the triangulated domain $\Omega_{h,t}$by $h_t := \{h_{K,t} : K \in T_{h,t}\}$. Suppose $V_h \subset V_A(\Omega_t)$, and $Q_h \subset Q_A(\Omega_t)$, is a conforming finite element (finite-dimensional) space. Let $\phi_h := \{\phi_i(x)\}$, $i = 1, 2, \ldots, N$, be the finite element basis functions of V_h. For the discrete form of the Navier-Stokes equation to have a stable solution, the discrete function spaces have to satisfy the so called Inf sup condition [12], [14], [6].

Hypothesis: (Uniform inf-sup condition) There exists a positive constant β1 independent of the discretisation parameter h such that

$$\inf_{q_h \in Q_h} \sup_{\mathbf{v}_h \in V_{h,0}} \frac{b_h(q_h, \mathbf{v}_h)}{||q_h||_0 |\mathbf{v}_h|_{1,h}} \geq \beta_1 > 0, \qquad (19)$$

Where

$$b_h(q_h, \mathbf{v}_h) = \sum_{K \in \mathcal{T}_h} \int_K q_h \nabla \cdot \mathbf{v}_h dx,$$

which is the pressure and velocity coupling in the Navier-Stokes equation

$$V_{h,0}(\Omega_t) = \{\mathbf{v}_h : \Omega \to \mathbb{R}^3,\ \mathbf{v}_h \in \mathrm{H}_0^1(\Omega_t)\} \text{ and,}$$
$$Q_h(\Omega_t) = \{q_h : \Omega_t \to \mathbb{R},\ q_h \in L_2(\Omega_t)\}.$$

The solution spaces for velocity and pressure have to be chosen in such a way that the condition (19) is satisfied. The following finite element pairs satisfy discrete inf-sup stable conditions on simplices with a constant β_1, which is independent of mesh parameter *h*.

1. continuous, piecewise polynomials of degree less than or equal to *k* for the velocity and continuous, piecewise polynomials of degree less than or equal to $k - 1$ for the pressure approximation, i.e., (p_k/p_{k-1}), for $k \geq 2$.

2. continuous piecewise polynomials of degree less than or equal to *k*, enriched with cell bubble functions for the velocity and discontinuous piecewise polynomials of degree less than or equal to $k - 1$ for the pressure approximation, i.e., $\frac{p_k^{bubble}}{p_{k-1}^{disc}}$ $for\ k \geq 2$.

3. continuous piecewise polynomials of degree less than or equal to *k*, $k = 2, 3$ in 2D for the velocity and discontinuous piecewise polynomials of degree less than or equal to $k - 1$ for the pressure approximation, i.e., $p_k/(p_{k-1} + p_0)$, for $k = 2, 3$.

4. On macro-element meshes, continuous piecewise polynomials of degree less than or equal to *k*, $k \geq 2$ in 2D and $k \geq 3$ in 3D, for the velocity and discontinuous piecewise polynomials of degree less than or equal to $k - 1$ for the pressure approximation i.e., (p_k/p_{k-1}^{disc}) for *k*, $k \geq 2$ in 2D and $k \geq 3$ in 3D, on macro element meshes.

The inf-sup stability proof of $\frac{p_k^{bubble}}{p_{k-1}^{disc}}, for\ k = 2, 3$ is given in [8]. The stability proofs of $p_k/(p_{k-1} + p_0)$, $k = 2, 3$ and $\frac{p_k}{p_{k-1}^{disc}}$, are presented in [16], [22] and [20], [21], [24] respectively. For the stability proof of all other finite element pairs p_k/p_{k-1}, $\frac{p_k^{bubble}}{p_{k-1}^{disc}}$, , we refer to [23] and the references given there.

We next define the semi discrete mesh velocity $\mathbf{w}_h$ in space using the semi discrete ALE mapping

$$\mathcal{A}_{h,t} : \hat{\Omega}_h \to \Omega_{h,t}. \tag{20}$$

Let

$$\mathcal{L}^1(\hat{\Omega}) = \left\{ \psi \in H^1(\hat{\Omega}) : \psi|_K \in \mathrm{P}_1(\hat{K}) \text{ for all } \hat{K} \in \hat{\Omega}_h \right\},$$

where P_1 is a set of polynomials of degree less than or equal to one on $\hat{K}$, be the piecewise linear Lagrangian finite element space. To move the mesh, it is sufficient to move the vertices, and thus the semi discrete (continuous in time) mesh velocity $\hat{w}_h(t, Y) \in L^1(\hat{\Omega})^d$ in the ALE frame for each $t \in [0, \mathrm{T})$ is defined as

$$\hat{\mathbf{w}}_h(t, Y) = \sum_{i=1}^{\mathcal{M}} \mathbf{w}_i(t)\psi_i(Y); \quad \mathbf{w}_i(t) \in \mathbb{R}^d.$$

Here, $\mathbf{w}_i(t)$ denotes the mesh velocity of the i^{th} node of simplices at $time\ t\ and\ \Psi_i(Y), i = 1, 2, \ldots . M,$ are the basis functions of $L^1(\hat{\Omega})$. We then define the semi-discrete mesh velocity in the Eulerian frame as

$$\mathbf{w}_h(t, x) = \hat{\mathbf{w}}_h \circ \mathcal{A}_{h.t}^{-1}(x).$$

Applying the finite element discretization to the NSE-ALE variational form (12), the semi- discrete form reads

$$\begin{aligned}
&\int_{\Omega(t)} \left.\frac{\partial \mathbf{u}_h}{\partial t}\right|_{\hat{\Omega}} \cdot \mathbf{v}_h \, dx + \int_{\Omega(t)} ((\mathbf{u}_h - \mathbf{w}_h) \cdot \nabla)\mathbf{u}_h \cdot \mathbf{v}_h \, dx + \frac{1}{\rho}\Big[2\mu \int_{\Omega(t)} \nabla_x(\mathbf{u}_h) : \mathbb{D}(\mathbf{v}_h) \, dx \\
&\qquad - \int_{\Omega(t)} (\nabla_x \cdot \mathbf{v}_h) \, p_h \, dx\Big] = \int_{\Omega(t)} \mathbf{g} \cdot \mathbf{v}_h \, dx + \frac{1}{\rho} \int_{\Gamma_F} \mathbf{v}_h \cdot \mathbf{r} \, dx, \quad \forall \ \mathbf{v}_h \in V_h(\Omega_t), \\
&\int_{\Omega(t)} (\nabla \cdot \mathbf{u}_h) q_h \, dx = 0, \ \forall \ q_h \in Q_h(\Omega_t).
\end{aligned} \tag{21}$$

4.1 Stability analysis of semi-discrete (continuous in time) NSE-ALE equation

Lemma 2 Stability of the semi-discrete problem: *Let the discrete version of* (9) *hold true. Then, the solution of the problem* (21) *satisfies*

$$\begin{aligned}
||u_h(t)||_{0,t}^2 + \int_0^T \int_{\Gamma_F} |\mathbf{u}_h|^2 (\mathbf{u}_h - \dot{\chi_F}) \cdot n \, dx \, dt + \kappa \int_0^T ||\nabla_x \mathbf{u}_h||_t^2 dt \\
\leq ||u_h(0)||_{0,t}^2 + \frac{2}{\kappa} \int_0^T \left[||g||_{0,t}^2 \, dt + \frac{1}{\rho} ||r(t)||^2 \right] dt.
\end{aligned}$$

To derive the stability estimates, take $v_h = u_h$ in (21), we obtain

$$\int_{\Omega(t)} \left.\frac{\partial \mathbf{u}_h}{\partial t}\right|_{\hat{\Omega}} \cdot \mathbf{u}_h \, dx + \int_{\Omega(t)} ((\mathbf{u}_h - \mathbf{w}_h)\cdot\nabla)\mathbf{u}_h \cdot \mathbf{u}_h \, dx + \frac{1}{\rho}\left[2\mu \int_{\Omega(t)} \nabla_x(\mathbf{u}_h) : \mathbb{D}(\mathbf{u}_h) \, dx - \int_{\Omega(t)} \nabla\cdot\mathbf{u}_h \, p_h \, dx\right]$$
$$+ \frac{1}{2}\int_{\Omega(t)} (\nabla\cdot\mathbf{u}_h)\mathbf{u}_h \, \mathbf{u}_h \, dx = \int_{\Omega(t)} \mathbf{g}\cdot\mathbf{u}_h \, dx + \frac{1}{\rho}\int_{\Gamma_F} \mathbf{u}_h \cdot \mathbf{r} \, dx, \quad \forall \ \mathbf{v}_h \in V_{h,0}(\Omega_t),$$
$$\int_{\Omega(t)} (\nabla\cdot\mathbf{u}_h) \, p_h \, dx = 0, \quad \forall \ q_h \in Q_h(\Omega_t).$$

We have made a modification to the equation above by including a consistent term $\left(\frac{1}{2}\int_{\Omega(t)} (\nabla\cdot\boldsymbol{u}_h)\boldsymbol{u}_h\boldsymbol{v}_h dx\right)$ to recover the stability estimates at the discrete level also. The first term can be written as

$$\int_{\Omega(t)} \left.\frac{\partial \mathbf{u}_h}{\partial t}\right|_{\hat{\Omega}} \cdot \mathbf{u}_h \, dx = \frac{1}{2}\frac{d}{dt}\int_{\Omega(t)} |\mathbf{u}_h|^2 \, dx - \frac{1}{2}\int_{\Gamma_F} \dot{\chi_F}\cdot n|u_h|^2 \, dx + \frac{1}{2}\int_{\Omega(t)} \mathbf{w}_h\cdot\nabla|u_h|^2 \, dx.$$

The second term can be split as

$$\int_{\Omega(t)} ((\mathbf{u}_h - \mathbf{w}_h)\cdot\nabla)\mathbf{u}_h \cdot \mathbf{u}_h \, dx = \frac{1}{2}\left[\int_{\Gamma_F} \mathbf{u}_h \cdot n|\mathbf{u}_h|^2 \, dx - \int_{\Omega(t)} \nabla\cdot(\mathbf{u}_h)|\mathbf{u}_h|^2 \, dx - \int_{\Omega(t)} \mathbf{w}_h\cdot\nabla|u_h|^2 \, dx\right]$$

Since $|u_h|^2 \notin Q_h(\Omega_t)$, the additional consistent term will be beneficial in eliminating the second term of the above equation. We emphasize the fact that this modification is consistent because the exact solution satisfies $\nabla\cdot\boldsymbol{u} = 0$. From here onwards, we will be taking into account the modified problem which includes the above-mentioned consistent term. By utilizing equation (13) with the value of $\kappa = 2\mu C_0$, and consolidating the previously mentioned factors, the resulting outcome is,

$$||u_h(t)||^2_{0,t} + \int_0^T \int_{\Gamma_F} |\mathbf{u}_h|^2(\mathbf{u}_h - \dot{\chi}_F)\cdot n \, dxdt + \kappa\int_0^T ||\nabla_x\mathbf{u}_h||^2_t dt$$
$$\leq ||u_h(0)||^2_{0,t} + \frac{2}{\kappa}\int_0^T \left[||f||^2_{0,t} \, dt + \frac{1}{\rho}||r(t)||^2\right]dt. \qquad (22)$$

In the semi-discrete case, the stability properties are affected by the domain velocity field. When the Neumann Boundary is set to zero, the apriori stability estimates for the Navier-Stokes equation in the ALE framework are the same as those in the fixed domain. This information can be inferred from the estimate provided above. Since the second term does not have a definite sign, the desired stability estimate can not be obtained. If $(\boldsymbol{u} - \dot{\chi}_F)\cdot n \geq 0, \forall\, x \in \Gamma_F^N$, the above estimate is stable. This happens when Γ_F^N is an outflow section means fluid exits the domain through the Neumann boundary Γ_F^N.

5. Time Stepping

In this section, we present the stability estimates for a fully discrete NSE-ALE form. In particular, the first-order modified implicit backward Euler time discretizations are analyzed. Let $0 = t_0 < t_1 < \cdots < t_N = I$ be a decomposition of the considered time interval [0, I]. Let us define $k_n = t_{n+1} - t_n, 0 \leq n \leq N-1$, be a sequence of timesteps.

5.1 Temporal discretization of ALE mapping

Since the ALE technique is used to handle the time-dependent domain, the domain velocity has to be provided at each instant t_n to discretize the Navier-Stokes equations in time. Therefore first we define the discrete (in time) domain velocity which is based on the ALE mapping. To define discrete (in time) ALE mapping, the reference

domain $\Omega^{\wedge}$ has to be defined. The choice of the reference domain is arbitrary, and often the initial domain Ω_0 is taken as the reference domain $\Omega^{\wedge}$. However, if the deformation of the domain Ω_t is very large in time, then it is appropriate to choose the latest available domain as the reference domain. Therefore we choose the previous timestep domain $\Omega_t n$ as the reference domain at the time interval $[t_n, t_{n+1}]$. Using this, we define the discrete in-time ALE mapping and the domain velocity at the interval $[t_n, t_{n+1}]$ as

$$\mathcal{A}_{n+1}^{n} : \Omega_{t_n} \to \Omega_{t_{n+1}}, \quad \mathbf{w}(\mathbf{x}, t) = \frac{\partial}{\partial t}(\mathbf{x}, t)$$

The finite element spaces for the velocity and the pressure using ALE extension in a moving domain on the time interval $[t_n, t_{n+1}]$ can be defined as

$$V_{\mathcal{A}_n}(\Omega_{t_{n+1}}) = \left\{ \mathbf{v}_{n+1} : \Omega_{t_{n+1}} \times [t_n, t_{n+1}] \to \mathbb{R}^3, \mathbf{v}_{n+1} = \hat{\mathbf{v}}_n \circ (\mathcal{A}_{n+1}^{n})^{-1}, \hat{\mathbf{v}}_n \in V(\hat{\Omega}_{t_n}) \right\}$$

$$V_{\mathcal{A}_n,0}(\Omega_{t_{n+1}}) = \left\{ \mathbf{v}_{n+1} : \Omega_{t_{n+1}} \times [t_n, t_{n+1}] \to \mathbb{R}^3, \mathbf{v}_{n+1} = \hat{\mathbf{v}}_n \circ (\mathcal{A}_{n+1}^{n})^{-1}, \hat{\mathbf{v}}_n \in V_0(\hat{\Omega}_{t_n}), \right.$$
$$\left. \mathbf{v}_{n+1} \cdot \boldsymbol{n} = 0 \text{ on } \Gamma_W \right\}$$

$$Q_{\mathcal{A}_n}(\Omega_{t_{n+1}}) = \left\{ q_{n+1} : \Omega_{t_{n+1}} \times [t_n, t_{n+1}] \to \mathbb{R}, \; q_{n+1} = \hat{q}_n \circ (\mathcal{A}_{n+1}^{n})^{-1}, \; \hat{q}_n \in Q(\hat{\Omega}_{t_n}) \right\}.$$

Fully implicit monolithic time discretization(one step): For a given fixedΩ_{t_n} , $\boldsymbol{u}_h^n \in V_h(\Omega_{t_n})$, $p_h^n \in Q_h(\Omega_{t_n})$, $\widehat{\boldsymbol{w}}_h^{n+1} \in H^1((A_{n+1}^n)^{-1}(\Omega_{t_{n+1}}))$, $find\ \widehat{\boldsymbol{u}}_h^{n+1} \in V_h(\Omega_{t_{n+1}})$, $\hat{p}_h^{n+1} \in Q_h(\Omega_{t_{n+1}})$, such that

$$\int_{\Omega(t_{n+1})} \frac{\hat{\mathbf{u}}_h^{n+1} - \mathbf{u}_h^n}{\Delta t} \cdot \mathbf{v}_h^{n+1} \, dx + \int_{\Omega(t_{n+1})} ((\hat{\mathbf{u}}_h^{n+1} - \hat{\mathbf{w}}_h^{n+1}) \cdot \nabla) \hat{\mathbf{u}}_h^{n+1} \cdot \mathbf{v}_h \, dx + \frac{1}{2} \int_{\Omega(t_{n+1})} (\nabla \cdot \mathbf{u}_h^{n+1}) \mathbf{u}_h^{n+1} \, \mathbf{u}_h^{n+1} \, dx$$
$$+ \frac{1}{\rho} \left[2\mu \int_{\Omega(t_{n+1})} \nabla_x(\mathbf{u}_h^{n+1}) : \mathbb{D}(\mathbf{u}_h^{n+1}) \, dx - \int_{\Omega(t_{n+1})} \nabla \cdot \mathbf{u}_h^{n+1} \, p_h^{n+1} \, dx \right]$$
$$= \int_{\Omega(t_{n+1})} g^{n+1} \cdot \mathbf{v}_h^{n+1} \, dx + \frac{1}{\rho} \int_{\Gamma_W(t_{n+1})} \mathbf{v}_h^{n+1} \cdot \mathbf{r} \, dx, \quad \forall \ \mathbf{v}_h^{n+1} \in V_{\mathcal{A}_n,0}(\Omega_{t_{n+1}}),$$
$$\int_{\Omega(t_{n+1})} (\nabla \cdot \hat{\mathbf{u}}_h^{n+1}) q_h^{n+1} \, dx = 0, \quad \forall \ q_h \in Q_{\mathcal{A}_n}(\Omega_{t_{n+1}}), \tag{23}$$

With the boundary condition as

$$\widehat{w}^{n+1} \cdot v_h = \widehat{\boldsymbol{w}}_h^{n+1} \cdot v \; on \; \Gamma_{F_{t_n}}$$

Remark: The computation of $\widehat{w}^{n+1}$ is discussed when linearization is discussed. The following identity holds for all $\psi_h \in V_{h,0}(\Omega_{h,t}), t \in (t_n t_{n+1}]$.

$$\int_{\Omega_t} \psi_h \nabla \cdot \mathbf{w}_h dx = \int_{\Omega_{t_n}} \hat{\psi}_h (J_{cof} \nabla \cdot) \hat{\mathbf{w}}_h dx$$

Where $\hat{\psi}_h \coloneqq \psi_h (A_{n+1}^n)^{-1}, \hat{w}_h = \boldsymbol{w}_h (A_{n+1}^n)^{-1}$ *and* J_{cof} is the cofactor of the Jacobian

Remark 1: In general an explicit of the form

$$\int_{\Omega_{t_{n+1}}} \psi_h \nabla \cdot \mathbf{w}_h^{n+1} dx \approx \int_{\Omega_{t_n}} \psi_h \nabla \cdot \mathbf{w}_h^{n+1} dx$$

has been used in all-time integration schemes, since the domain $\Omega_{t_{n+1}}$ is unknown a-priori, and therefore the calculation of the Jacobian J_{cof} is not possible.

5.2 Linearisation and solution process

Here we describe the linearisation process of the non-linear convection term in the weak form of the momentum balance equation of Navier-Stokes equations. It is based on a fixed point iteration type. As an example, consider the convection term at the time t_{n_2} on $[t_{n_1}, t_{n_2}]$. The non-linear convective term is then

$$\int_{\hat{\Omega}_{n_1}} (\mathbf{u}_h^{n_2} \cdot \nabla)\mathbf{u}_h^{n_2} \cdot \mathbf{v}_h \, dx, \tag{24}$$

where $\widehat{\Omega}_{n_1} := \left(A_{n_2}^{n_1}\right)^{-1} (\Omega_{t_{n_2}})$. This results in a system of nonlinear algebraic equations. In general, instead of solving a nonlinear system, the convection term is linearised and a linear algebraic system is solved for the Navier-Stokes equations.

In our computations, we prefer to use the fully implicit form of the convection term (24) with an iteration of fixed point type. The basic idea in the fixed point iteration is to iterate the entire system with some criterion at each time step. At the time t_{n_2}, we use an iteration $\boldsymbol{u}_l^{n_2} \rightarrow \boldsymbol{u}_{l+1}^{n_2}$based on

$$\int_{\hat{\Omega}_{t_{n_1}}} (\mathbf{u}_h^{n_2} \cdot \nabla)\mathbf{u}_h^{n_2} \cdot \mathbf{v}_h^{n_2} \, dx \approx \int_{\hat{\Omega}_{t_{n_1}}} (\mathbf{u}_{h,l}^{n_2} \cdot \nabla)\mathbf{u}_{h,l+1}^{n_2} \cdot \mathbf{v}_h^{n_2} \, dx,$$

with known $u_0^{n_2} (= u^{n_1})$. We iterate (25) for a fixed number of times or the residual becomes less than the prescribed value in each time step. It is clear that the fully implicit form with fixed point iteration is computationally more expensive than other time-stepping methods such as explicit or semi-implicit. However, the fully implicit form leads to a robust and stable solution, which is essential for moving domain problems. Thus

$$\begin{aligned}
&\int_{\Omega(t_{n+1})} \frac{\hat{\mathbf{u}}_{h,l+1}^{n+1} - \mathbf{u}_h^n}{\Delta t} \cdot \mathbf{v}_h \, dx + \int_{\Omega(t_{n+1})} ((\hat{\mathbf{u}}_{l,h}^{n+1} - \hat{\mathbf{w}}_{h,l}^{n+1}) \cdot \nabla)\hat{\mathbf{u}}_{h,l+1}^{n+1} \cdot \mathbf{v}_h \, dx + \frac{1}{2} \int_{\Omega(t_{n+1})} (\nabla \cdot \mathbf{u}_h^{n+1})\mathbf{u}_h^{n+1} \, \mathbf{v}_h^{n+1} \, dx \\
&\quad + \frac{1}{\rho} \left[2\mu \int_{\Omega(t_{n+1})} \nabla_x(\mathbf{u}_h^{n+1}) : \mathbb{D}(\mathbf{u}_h^{n+1}) \, dx - \int_{\Omega(t_{n+1})} \nabla \cdot \mathbf{u}_h^{n+1} \, p_h^{n+1} \, dx \right] \\
&\quad = \int_{\Omega(t_{n+1})} g^{n+1} \cdot \mathbf{v}_h^{n+1} \, dx + \frac{1}{\rho} \int_{\Gamma_W(t_{n+1})} \mathbf{v}_h^{n+1} \cdot \mathbf{r} \, dx, \quad \forall \ \mathbf{v}_h \in V_{\mathcal{A}_n,0}(\Omega_{t_n}), \\
&\int_{\Omega(t_{n+1})} \left(\nabla \cdot \hat{\mathbf{u}}_{h,l+1}^{n+1} \right) q_h \, dx = 0, \quad \forall \ q_h \in Q_{\mathcal{A}_n}(\Omega_{t_n}).
\end{aligned} \tag{26}$$

with $\widehat{\boldsymbol{w}}_{h,l}^{n+1}$ obtained from $\widehat{\boldsymbol{u}}_{h,l}^{n+1}$ by solving the linear elastic equation.

5.3 Stability estimates of the fully discrete NSE-ALE with Implicit Euler time discretization

For the sake of simplicity, we will use the suffix (l) only for the second nonlinear term. The equation can be written as

$$\begin{aligned}
&\int_{\Omega(t_{n+1})} \frac{\mathbf{u}_h^{n+1} - \mathbf{u}_h^n}{\Delta t} \cdot \mathbf{v}_h \, dx + \int_{\Omega(t_{n+1})} ((\hat{\mathbf{u}}_{h,l}^{n+1} - \hat{\mathbf{w}}_{h,l}^{n+1}) \cdot \nabla)\mathbf{u}_h^{n+1} \cdot \mathbf{v}_h \, dx + \frac{1}{2} \int_{\Omega(t_{n+1})} (\nabla \cdot \mathbf{u}_h^{n+1})\mathbf{u}_h^{n+1} \, \mathbf{v}_h^{n+1} \, dx \\
&\quad + \frac{1}{\rho} \left[2\mu \int_{\Omega(t_{n+1})} \nabla_x(\mathbf{u}_h^{n+1}) : \mathbb{D}(\mathbf{u}_h^{n+1}) \, dx - \int_{\Omega(t_{n+1})} \nabla \cdot \mathbf{u}_h^{n+1} \, p_h^{n+1} \, dx \right] \\
&\quad = \int_{\Omega(t_{n+1})} g^{n+1} \cdot \mathbf{v}_h^{n+1} \, dx + \frac{1}{\rho} \int_{\Gamma_F(t_{n+1})} \mathbf{v}_h^{n+1} \cdot \mathbf{r} \, dx, \quad \forall \ \mathbf{v}_h \in V_{\mathcal{A}_n,0}(\Omega_{t_n}), \\
&\int_{\Omega(t_{n+1})} (\nabla \cdot \hat{\mathbf{u}}_{l+1}^{n+1}) \, q_h \, dx = 0, \quad \forall \ q_h \in Q_{\mathcal{A}_n}(\Omega_{t_n})
\end{aligned} \tag{27}$$

Taking $v^h = u_h^{n+1}$, we get

$$\int_{\Omega(t_{n+1})} \frac{\mathbf{u}_h^{n+1} - \mathbf{u}_h^n}{\Delta t} \cdot \mathbf{u}_h^{n+1}\, dx + \int_{\Omega(t_{n+1})} ((\mathbf{u}_{h,l} - \mathbf{w}_{h,l}) \cdot \nabla)\mathbf{u}_h^{n+1} \cdot \mathbf{u}_h^{n+1}\, dx + \frac{1}{2}\int_{\Omega(t_{n+1})} (\nabla \cdot \mathbf{u}_h^{n+1})\mathbf{u}_h^{n+1}\ \mathbf{u}_h^{n+1}\, dx$$
$$+ \frac{1}{\rho}\left[2\mu \int_{\Omega(t_{n+1})} \nabla_x(\mathbf{u}_h^{n+1}) : \mathbb{D}(\mathbf{u}_h^{n+1})\, dx - \int_{\Omega(t_{n+1})} \nabla \cdot \mathbf{u}_h^{n+1}\, p_h^{n+1}\, dx\right]$$
$$= \int_{\Omega(t_{n+1})} g \cdot \mathbf{u}_h^{n+1}\, dx + \frac{1}{\rho}\int_{\Gamma_{F_{t_{n+1}}}} \mathbf{u}_h^{n+1} \cdot \mathbf{r}\, dx,$$

$$\int_{\Omega(t_{n+1})} (\nabla \cdot \mathbf{u}_h^{n+1})\, p_h^{n+1}\, dx = 0, \tag{28}$$

The second term can be written as

$$\int_{\Omega(t_{n+1})} ((\mathbf{u}_{h,l} - \mathbf{w}_{h,l}^{n+1}) \cdot \nabla)\mathbf{u}_h^{n+1} \cdot \mathbf{u}_h^{n+1}\, dx = \frac{\Delta t}{2}\left[-\int_{\Omega(t_{n+1})} \nabla \cdot (\mathbf{u}_{h,l} - \mathbf{w}_{h.l}^{n+1})|\mathbf{u}_h^{n+1}|^2\, dx\right.$$
$$\left. + \int_{\Gamma_F^{n+1}} (\mathbf{u}_{h,l}^{n+1} - \dot{\chi}_F^{n+1}) \cdot n|u_h^{n+1}|^2\, dx\right]$$

applying Cauchy-Schwarz inequality, we get

$$||\mathbf{u}_h^{n+1}||_{0,t^{n+1}}^2 + \int_{\Gamma_F^{n+1}} (\mathbf{u}_{h,l}^{n+1} - \dot{\chi}_F^{n+1}) \cdot n|u_h^{n+1}|^2\, dx + \frac{\Delta t}{2}\kappa||\mathbf{u}_h^{n+1}||_{t^{n+1}}^2$$
$$\leq -\frac{1}{2}\Delta t \int_{\Omega_{t^{n+1}}} \nabla \cdot \mathbf{w}_h^{n+1}|u_h^{n+1}|^2\, dx + \frac{1}{2}||\mathbf{u}_h^n||_{0,t^{n+1}}^2 + \frac{1}{2}||\mathbf{u}_h^{n+1}||_{0,t^{n+1}}^2 + \Delta t||g^{n+1}||_{0,t^{n+1}}^2 + \frac{1}{\rho}||r_{n+1}||_{0,t^{n+1}}^2.$$

From the Reynolds identity, we have

$$||\mathbf{u}_h^n||_{0,t^{n+1}}^2 = ||\mathbf{u}_h^n||_{0,t^n}^2 + \int_{t^n}^{t^{n+1}} \int_{\Omega_t} \nabla \cdot \mathbf{w}_h|\mathbf{u}_h^n|^2\, dx\, dt,$$

and we get

$$||\mathbf{u}_h^{n+1}||_{0,t^{n+1}}^2 + \int_{\Gamma_F^{n+1}} (\mathbf{u}_{h,l}^{n+1} - \dot{\chi}_F^{n+1}) \cdot n|u_h^{n+1}|^2\, dx + \frac{\Delta t}{2}\kappa||\mathbf{u}_h^{n+1}||_{t^{n+1}}^2$$
$$\leq \int_{t^n}^{t^{n+1}} \int_{\Omega_t} \nabla \cdot \mathbf{w}_h|\mathbf{u}_h^n|^2\, dx\, dt - \frac{\Delta t}{2}\int_{\Omega_{t^{n+1}}} \nabla \cdot \mathbf{w}_h^{n+1}|\mathbf{u}_h^{n+1}|^2\, dx + ||\mathbf{u}_h^n||_{0,t^n}^2 + \Delta t\frac{2}{\kappa}||g^{n+1}||_{0,t^{n+1}}^2$$
$$+ \frac{\Delta t}{\rho}||r^{n+1}||_{0,t^{n+1}}^2.$$

Let

$$\mathcal{A}_{t_n,t_{n+1}} = \mathcal{A}_{t_{n+1}} \circ \mathcal{A}_{t_n}^{-1}$$

be the ALE mapping between Ω_{t_n} and $\Omega_{t_{n+1}}$, and $J_{A_{t_n,t_{n+1}}}$ be it Jacobian. Then we have

$$||\mathbf{u}_h^{n+1}||^2_{0,t^{n+1}} + \int_{\Gamma_F^{n+1}} (\mathbf{u}_{h,l}^{n+1} - \dot{\chi}_F^{n+1}) \cdot n|u_h^{n+1}|^2 \, dx + \frac{\Delta t}{2}\kappa||\mathbf{u}_h^{n+1}||^2_{t^{n+1}}$$
$$\leq \Delta t||\nabla \cdot \mathbf{w}_h(t^{n+1})||_{\infty,t^{n+1}}||\mathbf{u}_h^{n+1}||^2_{0,t^{n+1}} + \Delta t\frac{2}{\kappa}||g^{n+1}||^2_{0,t^{n+1}}$$
$$+ \left(1 + \Delta t \sup_{t\in(t^n,t^{n+1})} ||J_{\mathcal{A}_{t_n,t_{n+1}}} \nabla \cdot \mathbf{w}_h||_{\infty,t}\right) ||\mathbf{u}_h^n||^2_{0,t^n} + \frac{\Delta t}{\rho}||r^{n+1}||^2_{0,t^{n+1}}.$$

Further, using the notation

$$\alpha_1^n = ||\nabla \cdot \mathbf{w}_h(t^n)||_{\infty,t^n}, \qquad \alpha_2^n = \sup_{t\in(t^n,t^{n+1})} ||J_{\mathcal{A}_{t_n,t_{n+1}}} \nabla \cdot \mathbf{w}_h||_{\infty,t},$$

The above equation can be written as

$$||\mathbf{u}_h^{n+1}||^2_{0,t^{n+1}} + \int_{\Gamma_F^{n+1}} (\mathbf{u}_{h,l}^{n+1} - \dot{\chi}_F^{n+1}) \cdot n|u_h^{n+1}|^2 \, dx + \frac{\Delta t}{2}\kappa||\mathbf{u}_h^{n+1}||^2_{t^{n+1}}$$
$$\leq \Delta t\alpha_1^{n+1}||\mathbf{u}_h^{n+1}||^2_{0,t^{n+1}} + (1 + \Delta t\alpha_2^n) ||\mathbf{u}_h^n||^2_{0,t^n} + \Delta t\frac{2}{\kappa}||g^{n+1}||^2_{0,t^{n+1}} + \frac{\Delta t}{\rho}||r^{n+1}||^2_{0,t^{n+1}}.$$

Summing over the index as i = 0, 1, 2, . . . , n, and assuming there is an outflow in the domain, the second term becomes positive, leading us to the following inequality:

$$||\mathbf{u}_h^{n+1}||^2_{0,t^{n+1}} + \frac{\Delta t}{2}\kappa||\mathbf{u}_h^{n+1}||^2_{t^{n+1}}$$
$$\leq \Delta t\alpha_1^{n+1}||\mathbf{u}_h^{n+1}||^2_{0,t^{n+1}} + \Delta t\sum_{i=1}^{n}(\alpha_1^i + \alpha_2^i)||\mathbf{u}_h^i||^2_{0,t^i} + (1 + \Delta t\alpha_2^0)||\mathbf{u}_h^0||^2_{0,t^0}$$
$$+ 2\frac{\Delta t}{\rho}\sum_{i=1}^{n+1}||r^i||^2_{0,t^i} + \Delta t\sum_{i=1}^{n+1}\frac{2}{\kappa}||g^i||^2_{0,t^i}$$
$$\leq \Delta t\sum_{i=1}^{n+1}(\alpha_1^i + \alpha_2^i)||\mathbf{u}_h^i||^2_{0,t^i} + (1 + \Delta t\alpha_2^0)||\mathbf{u}_h^0||^2_{0,t^0} + \sum_{i=1}^{n+1}\Delta t\left(\frac{2}{\kappa}||g^i||^2_{0,t^i} + \frac{1}{\rho}||r^i||^2_{0,t^i}\right).$$

$$||\mathbf{u}_h^{n+1}||^2_{0,t^{n+1}} + \frac{\Delta t}{2}\kappa||\mathbf{u}_h^{n+1}||^2_{t^{n+1}}$$
$$\leq \Delta t\alpha_1^{n+1}||\mathbf{u}_h^{n+1}||^2_{0,t^{n+1}} + \Delta t\sum_{i=1}^{n}(\alpha_1^i + \alpha_2^i)||\mathbf{u}_h^i||^2_{0,t^i} + (1 + \Delta t\alpha_2^0)||\mathbf{u}_h^0||^2_{0,t^0}$$
$$+ 2\frac{\Delta t}{\rho}\sum_{i=1}^{n+1}||r^i||^2_{0,t^i} + \Delta t\sum_{i=1}^{n+1}\frac{2}{\kappa}||g^i||^2_{0,t^i}$$
$$\leq \Delta t\sum_{i=1}^{n+1}(\alpha_1^i + \alpha_2^i)||\mathbf{u}_h^i||^2_{0,t^i} + (1 + \Delta t\alpha_2^0)||\mathbf{u}_h^0||^2_{0,t^0} + \sum_{i=1}^{n+1}\Delta t\left(\frac{2}{\kappa}||g^i||^2_{0,t^i} + \frac{1}{\rho}||r^i||^2_{0,t^i}\right).$$

We now apply Gronwall's lemma to get

$$\|\mathbf{u}_h^{n+1}\|^2_{0,t^{n+1}} + \frac{\Delta t}{2}\kappa \sum_{i=1}^{n+1} ||\mathbf{u}_h^i(t)||^2_{t^i} \leq$$

$$\leq \left[(1+\Delta t\alpha_2^0)\|\mathbf{u}_h^0\|^2_{0,t^0} + \Delta t \sum_{i=1}^{n+1}\left(\frac{2}{\kappa}\|g^i\|^2_{0,t^i} + \frac{1}{\rho}||r^i||^2_{0,t^i}\right)\right] \exp\left(\Delta t \sum_{i=1}^{n+1} \frac{\alpha_1^i + \alpha_2^i}{1-\Delta t(\alpha_1^i+\alpha_2^i)}\right)$$

The above stability estimate is stable provided we have

$$\Delta t < \frac{1}{\alpha_1^n + \alpha_2^n} = \left(\|\nabla \cdot \mathbf{w}_h(t^n)\|_{\infty,t^n} + \sup_{t\in(t^n,t^{n+1})} \|J_{A_{t^n,t^{n+1}}} \nabla \cdot \mathbf{w}_h\|_{\infty,t}\right)^{-1}$$

6. Implementation and numerical results

A test example of a rectangular fluid tank is taken with dimensions 1m in length, 0.4m in width, and the mean height of the fluid as 0.3m. A sinusoid is taken as the initial height profile of a free surface with amplitude $0.03m$ and spatial frequency $1Hz$ by linearly joining a sine waveform on one longitudinal edge and cosine(sine with a shift of 90^0) waveform on the other longitudinal edge. The profile is given as $y = \frac{(z-0.4)}{0.4}(0.3 + 0.03sin(2\pi x)) + \frac{z}{0.4}(0.3 + 0.03cos(2\pi x))$. This would cause imbalance in body forces and thus induces motion. The fluid properties, density is taken as 500 kg/m^3, dynamic viscosity as $0.89Pa.s$, and gravitational constant is taken as $9.8m/s^2$. The external traction at Γ_F (t) i.e., **r** is taken as zero. The domain is discretized as a transfinite mesh with 1539 hexahedrons. A p_2/p_1 element is used for velocity/pressure in Navier-Stokes equations which satisfies the inf-sup condition which results in 42237 velocity degrees of freedom(for three components)and 2000 pressure degrees of freedom. A p_1 element is used for mesh velocity in a linear elastic model which gives 6000 mesh velocity degrees of freedom. Figure 3 shows the computational domain at $t = 0$. Figure 6 shows the free surface at times 0.5s, 1.0s, 2.0s, and 4.0s respectively. The open source package deal.ii [3] which stands for 'Differential equations analysis library', which is a set of subroutines/classes for Finite element workflow is used. The library is written in C++ programming language and parallelization is based on MPI (Message passing interface). The FE package deal.ii can interface with various other MPI-based packages such as 'p4est' [7] for domain decomposition and 'petsc' [18] and 'mumps' [2] for linear algebra/matrix solution process. The finite element mesh is generated by Gmsh [11] and visualization in Paraview [1]. The code was implemented on 64 AMD EPYC cores on 4 interconnected nodes and took a wallclock time of 12 hours for 400 time steps.

.

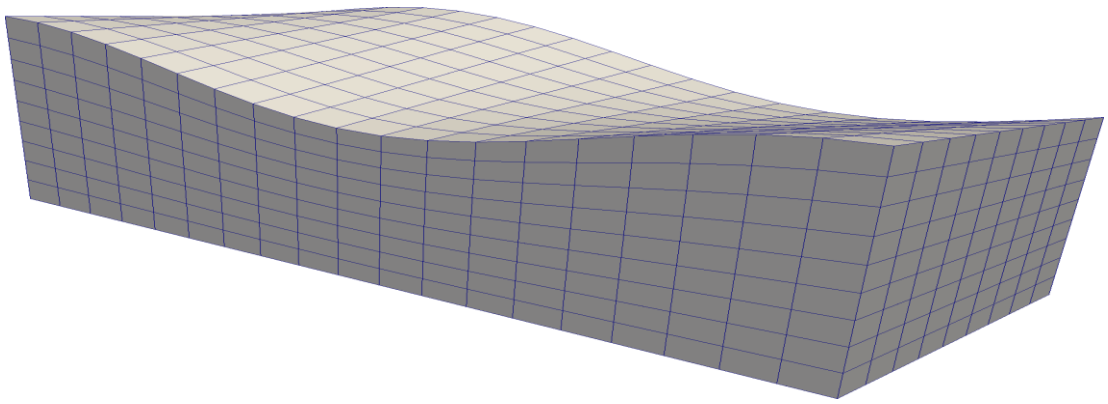

Fig.3 Discretised domain with initial uneven free surface.

As described in section 5, a fully implicit time discretization is employed with a time step of 0.01s. The simulation is carried out for a total of five seconds, i.e., 500 timesteps. The simulation was stable throughout. Table 1 shows the mass of the computational domain at various timesteps. In a span of 500 timesteps, a 1.30% of the total mass

is lost, which is well within acceptable limits. Table 2 shows the total mechanical energy (kinetic and potential) of the flow at various timesteps. It can be inferred from the table that the total mechanical energy monotonically decreases with time which is a nature of viscous flow and thus shows the stable nature of the scheme. Finally, figure 6 shows the result of the simulation, i.e., the free surface profile at times 0.5s, 1.0s, 2.0s, and 4.0s, respectively

Table.1 Volume of the computational domain at various timesteps

Time(s)	Volume(m^3)	Vt+0.5 − Vt(m^3)	% loss from initial volume
0	0.120003	-	0
0.5	0.119393	-6.10e-4	0.53
1.0	0.119368	-2.50e-5	0.55
1.5	0.119212	-1.56e-5	0.68
2.0	0.119236	2.40e-5	0.66
2.5	0.119059	-1.77e-4	0.80
3.0	0.118895	-1.64e-4	0.94
3.5	0.118801	-9.50e-5	1.02
4.0	0.118656	-1.45e-4	1.14
4.5	0.118557	-9.90e-5	1.22
5.0	0.118460	-9.7e-5	1.30

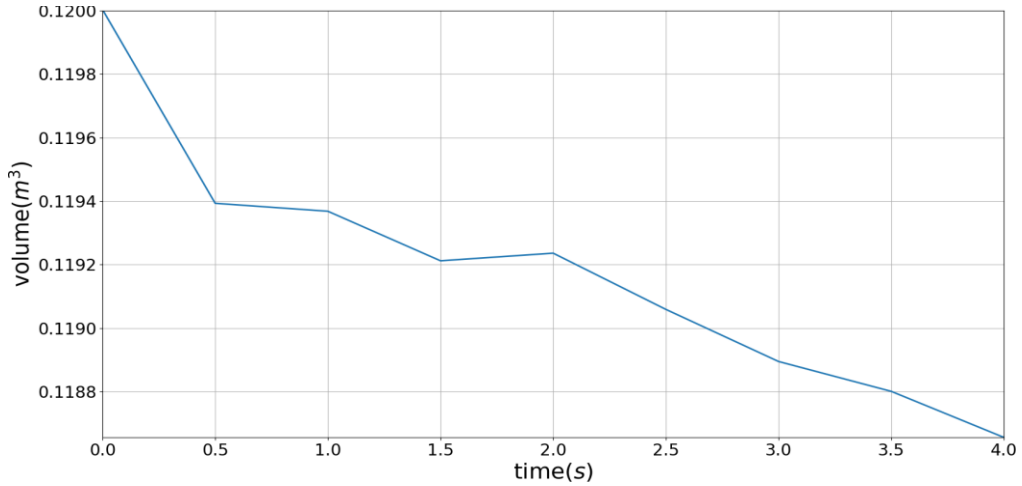

Fig.4 Volume of the fluid at various timesteps

Table.2 Total energy of the flow at various timesteps

Time(s)	Total energy(10*J*)
0	9.97
0.5	8.71
1.0	7.85
1.5	7.41
2.0	7.20
2.5	7.13
3.0	7.08
3.5	7.08
4.0	7.07
4.5	7.03
5.0	7.02

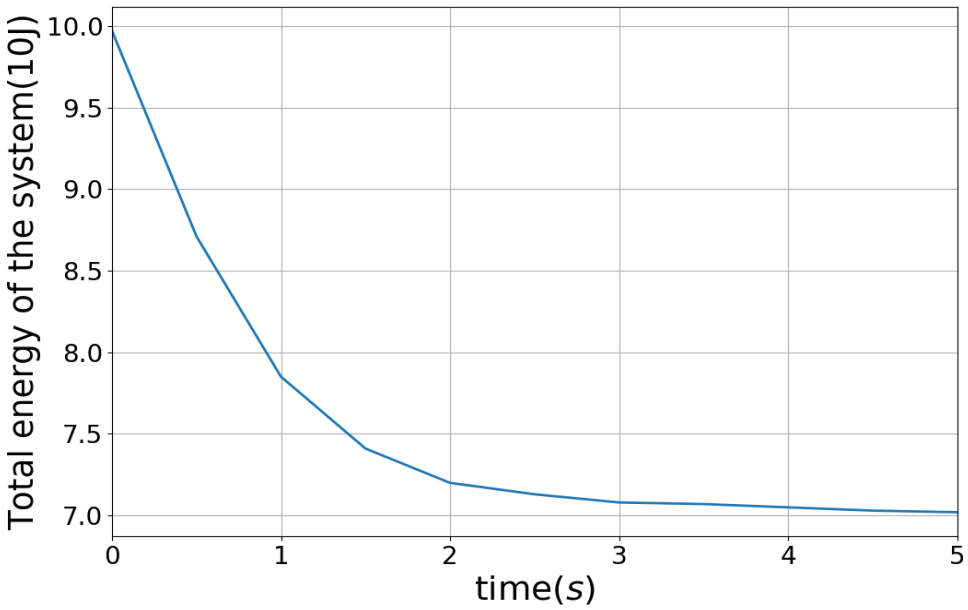

Fig.5 Total mechanical energy in the system at various timesteps

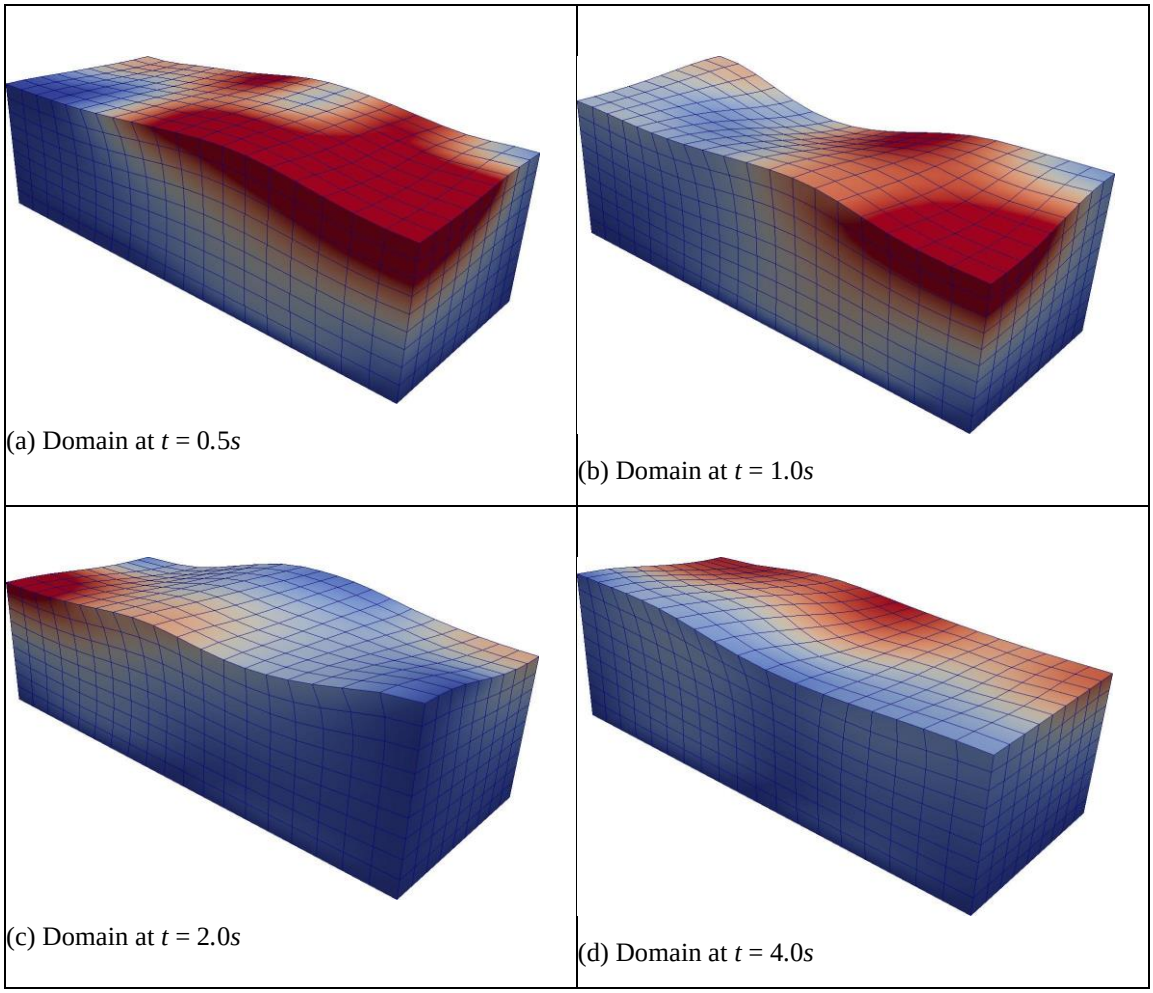

(a) Domain at $t = 0.5s$

(b) Domain at $t = 1.0s$

(c) Domain at $t = 2.0s$

(d) Domain at $t = 4.0s$

Fig.6 Free surface profile at 0.5s, 1.0s, 2.0s and 4.0s respectively

7. Conclusion

In this paper, we elaborate the ALE method for moving domain problems including a well- described inclusion of boundary conditions in weak form and time stepping. The stability estimates for the proposed NSE-ALE scheme are derived. It is shown that the stability of the semi-discrete (continuous in time) NSE-ALE equation is independent of the mesh velocity provided if it is an outflow through the Neumann boundary. Whereas the stability of the fully discrete scheme with the implicit Euler time discretization is only conditionally stable (time step depends on mesh velocity). We applied it to a test case of fluid sloshing in a rectangular tank. We have demonstrated the scheme and the simulation is stable for several timesteps. Particularly the scheme has shown very good mass/volume conservation properties. Thus it shows that the ALE approach for moving domain problems along with implicit Euler time-stepping schemes has very good mass conservation properties in applications with small topological changes.

Conflict of interest

The authors declare that they have no conflict of interest.

References

[1] Ahrens, James, Geveci, Berk, Law, Charles: Paraview: An end-user tool for large data visualization, visualization handbook. Visualization Handbook (ISBN-13: 978-0123875822) (2005)

[2] Amestoy, P., Duff, I.S., Koster, J., L'Excellent, J.Y.: A fully asynchronous multifrontal solver using distributed dynamic scheduling. SIAM Journal on Matrix Analysis and Applications 23(1), 15–41 (2001)

[3] Arndt, D., Bangerth, W., Davydov, D., Heister, T., Heltai, L., Kronbichler, M., Maier, M., Pelteret, J., Turcksin, B., Wells, D.: The deal.ii finite element library. CoRR abs/1910.13247 (2019). URL http://arxiv.org/abs/1910.13247

[4] Azzeddine Soulaimani, Y.S.: An arbitrary Lagrangian-Eulerian finite element method for solving three-dimensional free surface flows. Computer methods in applied mechanics and engineering 162, 79–106 (1998)

[5] Baskok, G.K.A., Aluru, N.: Microflows and Nanoflows. Springer (2005)

[6] Bathe, K.J.: The inf sup condition and its evaluation for mixed Finite element methods. Computers and structures 79, 243–252 (2001)

[7] Burstedde, C., Wilcox, L.C., Ghattas, O.: p4est: Scalable algorithms for parallel adaptive mesh refinement on forests of octrees. SIAM Journal on Scientific Computing 33(3), 1103–1133 (2011). DOI 10.1137/100791634

[8] Crouzeix, M., Raviart, P.A.: Conforming and nonconforming finite element methods for solving the stationary Stokes equations i. ESAIM: Mathematical Modelling and Numerical Analysis - Modelisation Mathematique et Analyse Num´erique 7(R3), 33–75 (1973)

[9] Don´ea, J.: Arbitrary Lagrangian Eulerian finite element methods. Computational methods for transient analysis pp. 473–516 (1983)

[10] Ganesan, S.: Finite element methods on moving meshes for free surface and interface flows. Ph.D. thesis, Otto-von-Guericke university, Germany (2006)

[11] Geuzaine, Christophe and Remacle, Jean-Francois: Gmsh. URL http://http://gmsh.info/

[12] Girault, V., Raviart, P.: Finite element methods for Navier Stokes equations. Springer-Verlag (1986)

[13] G.Tryggvason, B.Bunner, A.Esmaeeli, D.Jurie, N.Al-Rawahi, W.Tauber, J.Han, S.NAs, Y.J.Jan: A front tracking method for the computations of multiphase flow. Journal of Computational Physics 169(2), 465–502 (2004)

[14] Hartmann, F.: The discrete Babuˇska-Brezzi condition. Archive of Applied Mechanics 56, 221–228 (1986)

[15] Hirt, C., Nichols, B.: Volume of fluids method for the dynamics of free boundaries. Journal of Computational Physics 39, 201–225 (1981)

[16] JiangXiaoliang, J., Cheng, C.: Stability of locally mass-conserving higher order Taylor-Hood elements. Journal of Systems Science and Mathematical Sciences 17, 193–197 (1997)

[17] McKee, S., Tom´e, M., Ferreira, V., Cuminato, J., Castelo, A., Sousa, F., Mangiavacchi, N.: The MAC method. Computers and Fluids 37(8), 907–930 (2008). DOI https://doi.org/10.1016/j.compfluid.2007.10.006. URL https://www.sciencedirect.com/science/article/pii/S0045793007001909

[18] Mills, R.T., Adams, M.F., Balay, S., Brown, J., Dener, A., Knepley, M., Kruger, S.E., Morgan, H., Munson, T., Rupp, K., Smith, B.F., Zampini, S., Zhang, H., Zhang, J.: Toward performance-portable PETSc for GPU-based exascale systems. Parallel Com- puting 108, 102831 (2021). DOI https://doi.org/10.1016/j.parco.2021.102831. URL https://www.sciencedirect.com/science/article/pii/S016781912100079X

[19] Osher, S., ASethian, J.: Fronts propagating with curvature-dependent speed: Algorithms based on Hamilton- Jacobi formulations. Journal of Computational Physics 79, 12–49 (1988)

[20] Scott, L.R., M.Vogelius: Conforming Finite Element Methods for Incompressible and Nearly Incompressible Continua. Large scale computations in fluid mechanics, Proceedings of 15th AMS-SIAM Summer seminar 22, 221–244 (1985)

[21] Scott, L.R., Vogelius, M.: Norm estimates for a maximal right inverse of the divergence operator in spaces of piecewise polynomials. ESAIM: Mathematical Modelling and Numerical Analysis - Modelisation Math´ematique et Analyse Num´erique 19(1), 111–143 (1985)

[22] Thatcher, R.W.: Locally mass-conserving Taylor–Hood elements for two- and three-dimensional flow. Inter- national Journal for Numerical Methods in Fluids 11, 341–353 (2005)

[23] V, G., Raviart: Finite element methods for Navier Stokes equations. Springer series in Computational Mathematics, Springer, New York (1986)

[24] Zhang, S.: A new family of stable mixed finite elements for the 3d stokes equations. Mathematics of Computation 74, 543–554 (2005)